ORIGINAL ARTICLE

Environmentally sustainable mining: a case study on surface subsidence control of grouting into overburden

Hewen Ma[1] · Wanghua Sui[2] · Jianming Ni[3]

Abstract

This paper presents an investigation on the effect of grouting into multi-bed-separation to control mining-induced surface subsidence. In the overburden without obvious thick-and-hard strata for generating large-scale bed separation, overburden grouting is carried out by increasing the number of boreholes and grouting strata. The scale model test, numerical simulation, and field measurements are used to study distribution and process of bed separation and to compare the overburden failure with surface subsidence due to pre- and post-overburden grouting, with a case study of the Qi'nan Coal Mine, Anhui Province, China. The scale model test and numerical simulation results of the overburden grouting process are in close agreement with those obtained from the field measurements. Filling masses with different diffusion radii are commonly formed in the different bed separation, which are overlaid to control the surface subsidence. It is proven that overburden grouting can successfully mitigate overburden failure and subsidence without obvious hard strata and bed separations. This provides an effective and cost-efficient approach for addressing the surface subsidence and overburden deformation problems due to mining.

Keywords Subsidence control · Bed separation · Grouting · Overburden failure · Numerical simulation · Scale model test

Introduction

Surface subsidence is an increasingly serious problem during coal mining operations performed under buildings, railways, and water bodies, and it may cause the destruction of fertile lands, damage to ground buildings (Bell et al. 2000; Loupasakis et al. 2014; Xuan and Xu 2014; Luan et al.

✉ Wanghua Sui
suiwanghua@cumt.edu.cn

Hewen Ma
mahewen@cumt.edu.cn

Jianming Ni
13605615852@163.com

[1] Institute of Mine Water Hazards Prevention and Controlling Technology, School of Resources and Geosciences, China University of Mining and Technology, 1 University Rd, Xuzhou 221008, Jiangsu, China

[2] Institute of Mine Water Hazards Prevention and Controlling Technology, School of Resources and Geosciences, China University of Mining and Technology, 1 University Rd, Xuzhou 221116, Jiangsu, China

[3] Huaibei Mining Group Co., Ltd, 276 Mid Renmin RD, Huaibei 235000, Anhui, China

2017). Strip and filling mining are commonly and effectively used in underground mining (Sroka et al. 2015; Yin et al. 2018; Jaiswal and Shrivastva 2012). However, filling method developed rapidly compared to other mining methods in recent years (Zhu et al. 2016; Zhang et al. 2011; Karfakis et al. 1996). There are two main options to fill mined-out area to mitigate surface subsidence and protect mine environment; goaf filling and overburden filling in accordance with filling locations. Filling mining method can be divided into gangue filling, sand filling, paste filling and high-water materials filling (Yao et al. 2012; Li et al. 2017; Yang and Li 2017; Belem and Benzaazoua 2008; Chang et al. 2018). Overburden grouting is another filling method carried out in bed separations.

With the rapid development and application of underground backfill mining, paste backfill mining techniques are widely used all over the world. Paste backfilling mining uses slurry made of aggregates such as fly ash or cement fill and water. The method was first implemented at the Preussag's Bad Grund Mine in Germany in 1979 and then applied to Australia (Rankine et al. 2007; Rankine and Sivakugan 2007; Sivakugan et al. 2015). Subsequently, it was gradually applied to control surface subsidence in many coal mines (Liu et al. 2017).

Overburden grouting is a relatively new method to control surface subsidence. The filling material is injected into the bed separation during mining by the vertical drilling boreholes. Bed separation occurs between different strata where the upper stratum is stronger than the lower one over the longwall excavation (Palchik 2003, 2005). The injected materials by a high pressure formed a certain size of pack to support the overlying strata. The compacted slurry injected into bed separation has a positive effect to support overburden and mitigate its deformation. It effectively controls and mitigates the surface subsidence caused by coal mining. Overburden grouting trial for mitigating subsidence originated in Poland in 1980, where surface subsidence was reduced by 20–30% in comparison with that due to caving method (Palarski 1989). It was then introduced into China and Australia. Surface subsidence was reduced by 63–65% (namely subsidence reduction ratio) at the Laohutai Coal Mine, China (Chen et al. 2016). Subsidence reduction ratio varies between 36 and 65% in other coal mines such as Xinwen, Kailuan, Huaibei (Sun et al. 2008). The estimation shows that the maximum subsidence reduction ratio is close to 50% in case of overburden grouting above longwall panel in West Cliff Colliery in Australia (Chen and Hu 2009; Shen and Poulsen 2014). Other results also show that overburden grouting can be used to control surface subsidence and deformation caused by mining (Palarski 1989; Gray et al. 1998; Sivakugan et al. 2006; Siriwardane et al. 2003; Lokhande et al. 2005). However, the efficiency of subsidence controlling is quite different in different injection locations and geological conditions. For instance, grout injecting into bed separation closer to mining seam can achieve more subsidence reduction (Chen and Guo 2008). Furthermore, combining with coal pillars, overburden grouting can further improve grouting effectiveness. Besides, larger bed separation developed with overlying thick and hard rock strata (e.g., igneous sill) benefits more grouts injection (Xuan and Xu 2014, 2017; Xuan et al. 2014). Several successful trials show that the overburden stresses and strains due to mining are reduced and the surface subsidence reduction ratio was improved based on partial mining and specific geological condition (Xuan and Xu 2014; Xuan et al. 2014).

Above mentioned modifications about overburden grouting are based on increasing width of pillars, adjusting injection locations and geological condition options to improve surface subsidence reduction ratio. Pumping pressure through boreholes and strata pressure transmitted by injected filling mass from overlying strata result in a compacted rock mass between bed separation and roof. The compacted rock, filling mass and coal pillar commonly support overburden to improve its stabilization. A thick and strong rock strata in overburden (i.e., the key stratum) is advantageous to implement overburden grouting and better effectiveness of surface subsidence control (Xuan and Xu 2017). Those

previous researches have considerably helped in improving subsidence reduction ratio. However, in some cases without thick and strong strata, overburden grouting into a single bed separation is insufficient to meet the requirements of construction protection (Sun et al. 2008). Therefore, a multi-bed separation grouting method is proposed in this paper by increasing the number of grouting boreholes and locations to enhance the injection ratio to meet the surface subsidence controlling requirements. The multi-bed separation grouting is implemented from the lower stratum to the upper one in the vertical direction and along the mining direction, respectively. The aim of this study is to investigate the development of multi-bed separation, the mechanism of subsidence control and the effectiveness of multi-bed separation grouting into overburden without thick and strong strata.

Hydrogeological and engineering geological conditions

The Qi'nan Coal Mine is located in Suzhou City, Anhui Province, China (Fig. 1). It covers approximately 1.5 km² and has a designed capacity of 1.8 million tons per year. It was put into operation in 2000. The Qi'nan Coal Mine is located in the Huaibei plain with an inclination of 7°–15°.

The Qi'nan Coal Mine has a low curved monoclinic structure with an inclination angle of 12°–24°. The coal seams belong to gentle-inclined one with an average inclination of 15°. The rocks deposited in the mining area mainly consist of clastic sedimentary rocks. The rocks at the roof and floor of the Seam no. 3-2 have different strengths; sandstone, siltstone and mudstone belong to hard, medium–hard and soft rock according to the Code for Investigation of Geotechnical Engineering (Ministry of Housing and Urban-Rural Development of the People's Republic of China 2002), respectively. Aquifers in this mine include the Cenozoic porous aquifer, the Permian fissured sandstone aquifer, the Carboniferous Taiyuan Formation and the Ordovician karst fissured aquifer. Overall, the specific capacity of the aquifers ranges from 0.0004 to 0.0455 L/(s m). The normal groundwater inflow is 0.5–1 m³/h in some panel.

The panel applied overburden grouting is the first longwall panel with a width of 187 m beneath the part without buildings and a width of 127 m beneath the villages which should be protected. The average mining depth of the seam is 467 m. Its advancing length is 1000 m with a mining rate from 100 to 150 m/month. The strike direction of the panel is nearly north to south. The Seam no. 3-2 is located in the Permian Upper Shihezi Formation. The cutting height is about 4 m. The roof of the Seam no. 3-2 was mainly composed of mudstone and fine stone and siltstone. The average thickness of the unconsolidated formation above bedrocks is 280 m.
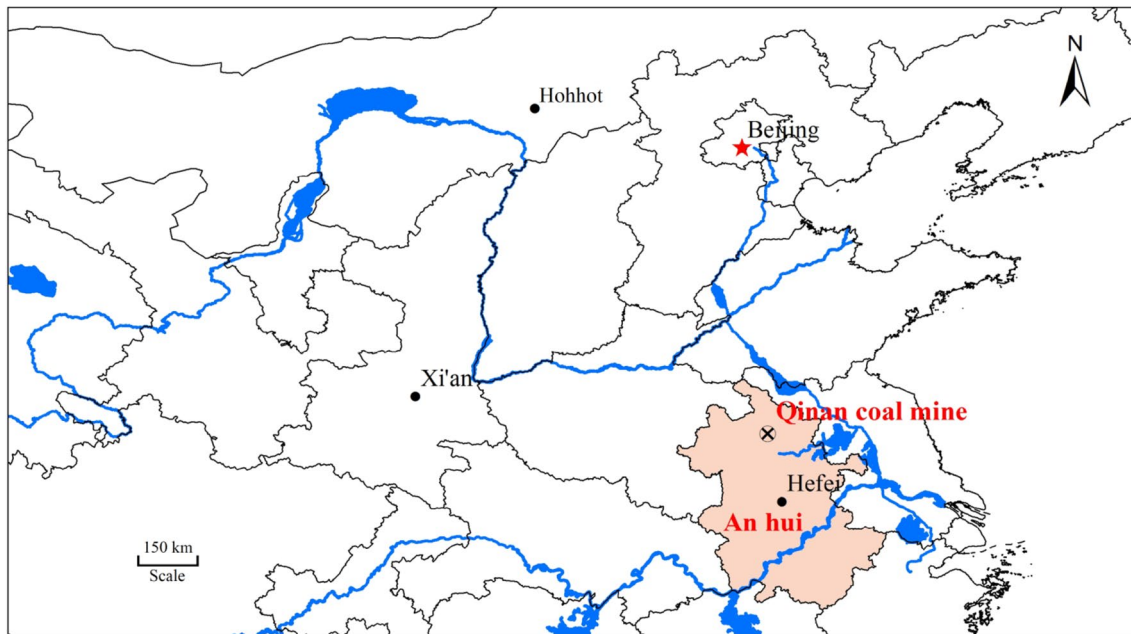
Fig. 1 Location of the Qi'nan Coal Mine

Method

Scale model testing

Scale model tests are carried out to investigate the development of multi-bed separation during mining and grouting into the bed separations for mitigating surface subsidence.

Table 1 lists the overburden stratigraphy and physico-mechanical parameters of rocks of the panel. The scale model has a size of 1.4 m × 0.2 m × 0.53 m (length × width × height) to a scale of 1:500. In the scale model, the overburden and the coal seam are simulated by a mixture of sand, calcium carbonate, gypsum, cement, pulverized coal and water. The mica was used to split the rock strata. The cutting height in the model was 0.8 cm on a buried depth of 93.4 cm representing the cutting height and buried depth of 4 m and 467 m in prototype, respectively (Fig. 2). Three observation lines and 27 monitoring points at 11.2, 15.4, and 21 cm were set from the roof of the coal seam, respectively. They represented observation lines were set at 56, 77, and 105 m in the prototype above the roof of the coal seam, respectively.

At the top of the model, three layers of iron bricks are used to simulate the gravitational pressure of the unconsolidated layer which is a distribution load of 9.45 kPa. The model tests simulate the mining process along the strike direction, excavating from right to left (Fig. 2). The open-off cut is excavated at a distance of 21 cm from the model boundary (Fig. 7a). The mining step is 7 cm, simulating the 35 m in prototype mining. The next excavation is performed

Table 1 Physico-mechanical properties of coal measures

| Lithology	Density (kg/m³)	Compressive strength (MPa)	Elastic modulus (MPa)	Internal friction angle (°)	Tensile strength (MPa)	Cohesion (MPa)	Poisson's ratio
Sandy mudstone	1700	–	1820	18	4.7	4.8	0.20
Fine sandstone	2700	37.8–84.6	2900	31	4.8	3.2	0.23
Siltstone	2500	40.6–72.5	2600–3600	35	4.8	4.4	0.24
Mudstone	2700	11.6–36.0	3000–4500	25	3.7	4.8	0.25
Medium sandstone	2600	67.0–88.1	6000	33	2.0	1.1	0.24
Seam no. 3-2	1400	–	1990	22	1.7	0.4	0.26
Sandstone	2600	105.4–219.4	50,000	33	3.0	3.1	0.14
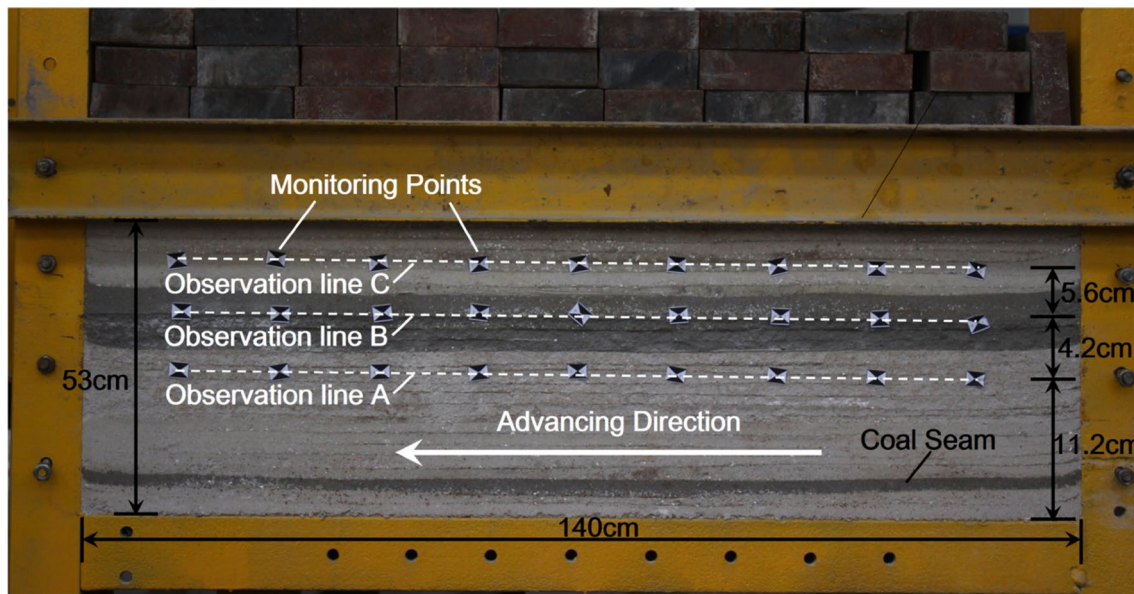
Fig. 2 A scale model to simulate subsidence and overburden grouting
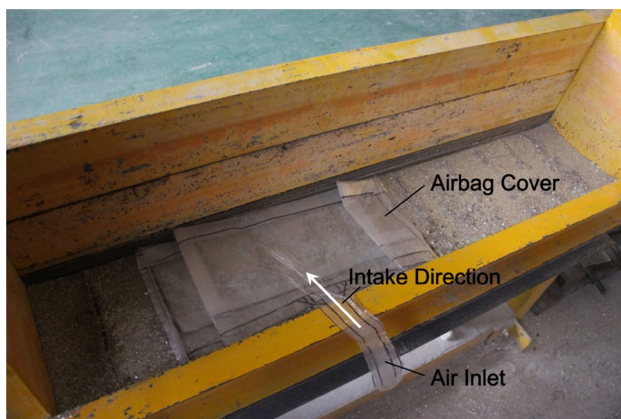

Fig. 3 Bed separation grouting simulated by injecting grout into a closed airbag

at an interval of about 15 min after the last excavation. The strata above the roof will break first during coal seam excavation simulation. The bed separation gradually develops from the roof of the coal seam to the ground surface in vertical direction and gradually develops horizontally along the excavation direction. Injection will be carried out while the separation occurred. The same excavation and injection sequence is carried out to bed separation repeatedly until mining completed.

The overburden grouting was simulated by an airbag and a micro-gas pump which is used to inject grouts into the airbag. The airbag was made of 0.2-mm-thick transparent polyethylene (PE) film and the expansion space was left inside the airbag (Fig. 3).

The average horizontal distance of observation points was 14 cm (70 m in prototype) and their locations and changes were obtained by photogrammetry. A boundary seam with a length of 21 cm was reserved on each side to offset the influence of the boundary effect. The simulated extraction distance was 98 cm (490 m in prototype).

Numerical simulation

Discrete element code UDEC is used to simulate the grouting into overburden with mining and analyze the relationship between the injection–production ratio and surface subsidence, as well as the grouting effect (Cundall and Strack 1979; Itasca Consulting Group, Inc 2005). This software has high-speed calculation performance and can complete large-scale accumulation model calculations. UDEC is based on a two-dimensional discrete element algorithm, which can describe the mechanical behavior of a discrete medium in two-dimensional space and can represent non-continuous media through simulating discrete blocks. UDEC's Fish language can be used to compile and calculate special functions such as overburden grouting.

Figure 4 shows the schematic diagram of 2D model. The simulated model size was set at 600 m × 472 m (length × height) and an excavation width of 127 m in accordance with the engineering geological and mining conditions for overburden bed separation grouting. There is a boundary of 236.5 m in both sides to reduce the boundary effect. Table 2 lists the mechanical properties of the overburden determined by laboratory testing. Moreover,
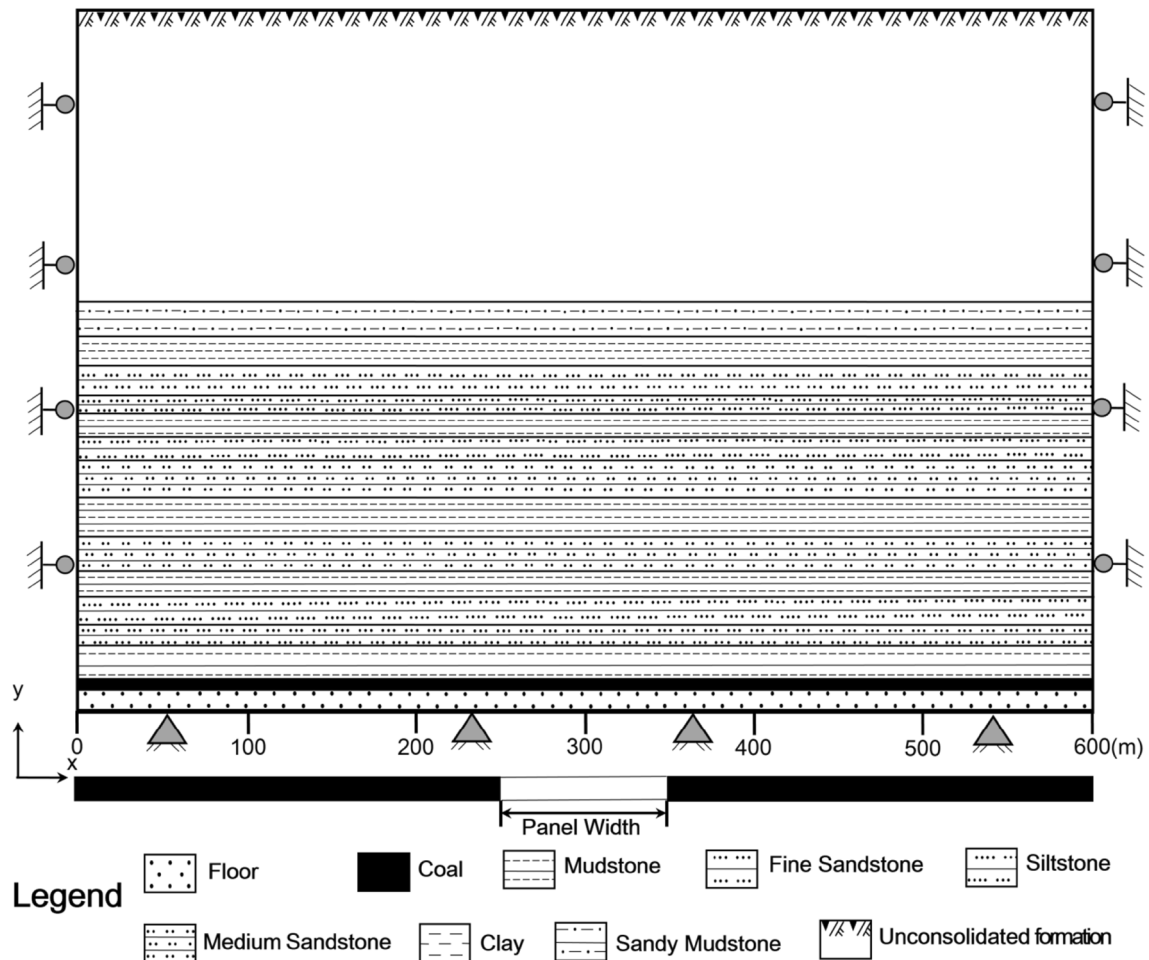
Fig. 4 Model geometries of UDEC numerical simulation

Table 2 Physico-mechanical properties of rock strata

Lithology	Density (kg/m³)	Bulk modulus (MPa)	Shear modulus (MPa)	Internal friction angle (°)	Tensile strength (MPa)	Cohesion (MPa)
Unconsolidated layer	1700	1010	760	18	4.7	1.6
Sandy mudstone	1700	1010	760	18	4.7	4.8
Clay	1700	1060	980	22	4.7	3.7
Fine sandstone	2600	1800	1200	31	4.8	3.2
Siltstone	2500	2600	1600	35	4.8	4.4
Mudstone	2700	2900	1800	25	3.7	4.8
Siltstone	2500	3600	2500	35	3.8	5.4
Medium sandstone	2600	3800	2400	33	2.0	1.1
Mudstone	2700	2000	1200	25	2.7	3.9
Medium sandstone	2600	3800	2400	33	2.0	1.1
Mudstone	2700	3100	1900	25	1.0	0.1
Siltstone	2500	1700	1000	35	1.1	0.2
Fine sandstone	2600	2000	1300	31	1.1	0.2
Mudstone	2700	2000	1200	25	1.0	0.1
Seam no. 3-2	1400	1400	790	22	1.7	0.4
Sandstone	2600	24,000	22,000	33	3.0	3.1

the boundary of the model is free at the top and fixed at the bottom and horizontal directions.

Field measurements

The slurry mix included the raw materials and solvent. In the grouting project, fly ash was used as the grouting aggregate mixing with a certain amount of water to make the filling slurry, which had strong diffusivity and fluidity. It filled the bed separation effectively using fewer drilling boreholes, and formed strong concretion. The water–cement mass and volume ratio of field grouting test was selected to be 1.4–2.5 and 1–1.4, respectively. The mixing ratio corresponded to the slurry concentration, which was represented by a ratio of water to aggregate by mass (abbreviated as W/C):

$$\rho^* = m_w/m_c, \qquad (1)$$

where ρ^* is the water–cement ratio, m_w is the mass of water, and m_c is the mass of fly ash.

The relationship between the slurry density and the W/C is given as follows:

$$\rho = \frac{\rho_c(\rho^* + 1)}{\rho_c\rho^* + 1}, \qquad (2)$$

where ρ_c is the density of fly ash.

After the fly ash slurry is injected, the water in the slurry will eventually lost (some of them infiltrates into surrounding

microcracks and some solidifies with cement slurry) and then the dry ash injected plays an effective role in reducing subsidence. Accordingly, W/C is properly adjusted to ensure the slurry has good fluidity in the filling space without considering the concretion rate and slurry controllability during the grouting.

To provide reliable measurements to study grouting effect, surface observation stations are set up on the surface above the panel to monitor the surface deformation and movement pre- and post-grouting. Figure 6 shows the layout of the observation stations. Three observation lines were set on the surface, including one in strike direction (labeled J1–J15) and two in dip direction (labeled J16–J34 and T1–T19, respectively).

Figure 5 shows the grouting pressure in different positions of the grouting system. The excessive water of slurry lost and solid components only leaves in the bed separation. This process will cause the changes of pressure in the bed separation.

When the grouting borehole pressure is larger than zero (P_o > 0), grouting pressure exists under the necessary conditions as follows: the bed separation is full of slurry and the volume of the grouting slurry is larger than the sum of the volume of the bed separation and the water outflow:

$$V_s > V_b + Q_w, \qquad (3)$$

where V_s is the grout take (m³/h), V_b is the volume of newly separated strata (m³/h), and Q_w is the volume of water flowing out of the bed separation (m³/h).
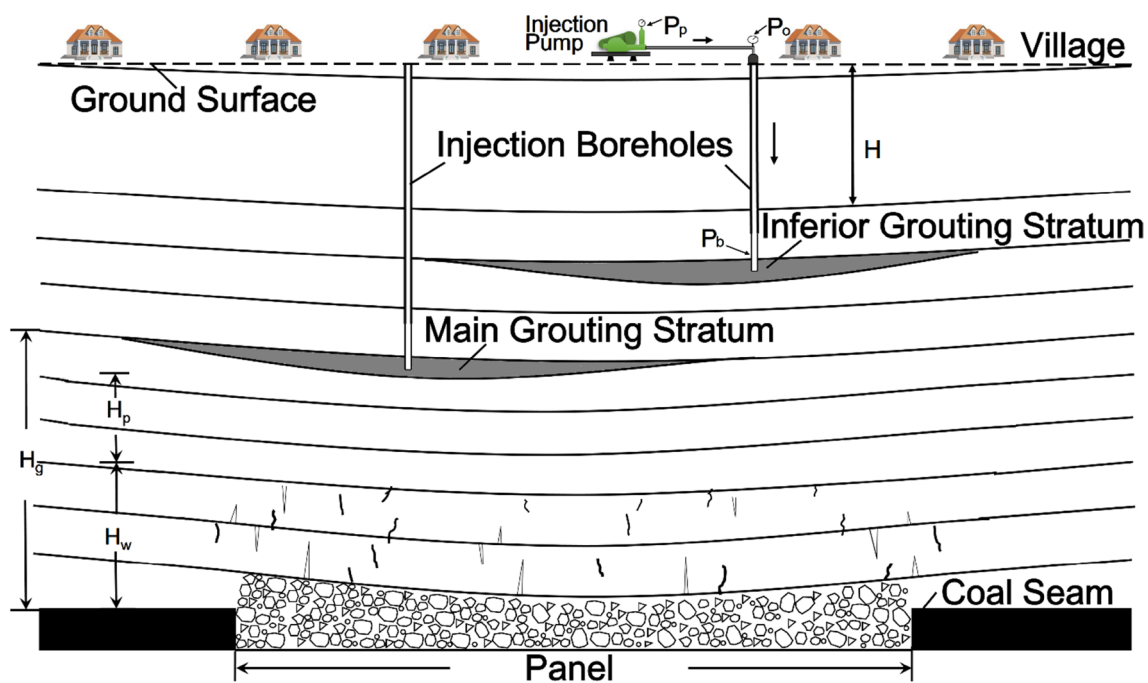

Fig. 5 Schematic of grout injection into overburden of isolated panel's longwall mining. P_o is the pressure of grouting pump; P_b the pressure inside bed separation; P_p the pump pressure; H the depth of bed separation; H_g the height of the grouting layer, H_w the height of the water-conducting fractured zone; H_p the height of the protective layer

In the grouting stage with pressure, the pressure inside separation space and for grouting pump is as follows:

$$P_o = P_p - H \times G_f - f_p, \tag{4}$$

$$P_b = P_p - H \times G_f - f_p + H \times \gamma_s, \tag{5}$$

where P_o is the pressure of grouting pump, P_b is the pressure inside bed separation, P_p is the pump pressure, H is the depth of bed separation, G_f is pressure gradient with depth, f_p is the resistance of grouting pipe and γ_s is the unit weight of slurry.

The grouting bed separations located in the range of strata which are above more than 10–20 m from the water-conducting fractured zone to ensure a safe grouting by preventing the panel from the injected slurry inrush. The main injection boreholes G1, G3, and G6 in the present experiment are 60 m from the roof of the coal seam and the auxiliary injection borehole G2, G4, and G5 is 90 m above the roof of the coal seam (Table 3 and Fig. 6).

Results and analysis

Mechanism of subsidence reduction with overburden grouting

The backfilling mass and its underlying strata in longwall backfill mining are reversed to support the overlying strata. However, in the case of overburden grouting, the filling mass between the rock masses above the panel transmits load to the lower rock through the strata under grouted bed separation. Eventually, the increased load is transmitted to the caving rocks which are then compacted.

The major difference between the two methods is that the compacted and supporting strata in the caving zone show a typically dynamic behavior under sufficient mining, in comparison, overburden grouting relies on the filling mass to expand and fill the space of bed separation during the process of grouting with a high-pressure and to compact directly the fractured rock in the condition of insufficient mining. Therefore, multi-bed separation overburden grouting can contribute to increase the volume of injected slurry and to improve grouting rate to control the surface subsidence.

Palchik (2005) proposed an empirical formula for development conditions of the bed separation:

$$K = \sqrt{M/H}\left[\ln\left(\sigma_a/\sigma_b\right) + \ln\left(h_a/h_b\right)\right] - a\left(h_d/h_a\right) > 0, \tag{6}$$

where M is the extraction height of coal seam; H is the distance of bed separation interface and extracted coal seam; σ_a and σ_b are the uniaxial compressive strengths of the upper and lower rock layer of the bed separation, respectively; h_a and h_b are the thickness of the upper and lower layer of the bed separation, respectively; and h_d is the thickness of the rock "layer-bridge" within the distance of 100 m from extracted coal seam. The coefficient a is equal to 0.07 in the formula. When the coefficient K is greater than zero, bed separation occurs. Here, the values of K of horizontal fracture are 0.25 and 0.23 calculated from the strata with a distance of 60 m and 90 m away from coal seam, respectively. It implies that the bed separation would occur between the rock mass with longwall mining.

The process of bed separation formation shows a cycle of "generation–development–expansion (persistence)–disappearance (compaction)". At the beginning, the bed separation appears as a horizontal fracture with the small size, and then it expands slowly until the upper boundary rock of the bed separation reached a critical breaking length. When the bed separation is close to the breaking length, the space of bed separation reaches the maximum at this moment. As the excavation continuing, the overburden deformation is intensified, the upper boundary rock of bed separation is bent downward and the space of bed separation gradually becomes smaller till closed. The process of bed separation development is repeated between the higher strata during excavation. Thus, the injected bed separation should have a safe distance from the water-conducting fractured zone to prevent he panel from injected slurry inrush. As a result, the locations for grouting should be higher than the sum of heights of water-conducting fractured zone and protective layer (Fig. 5):

$$H_{g\,min} = H_w + H_p, \tag{7}$$

where H_g is the height of the grouting layer, H_w is the height of the water-conducting fractured zone and H_p is the height of the protective layer. The protective layer is generally selected from 10 to 20 m.

Table 3 Designed locations and depths of grouting boreholes

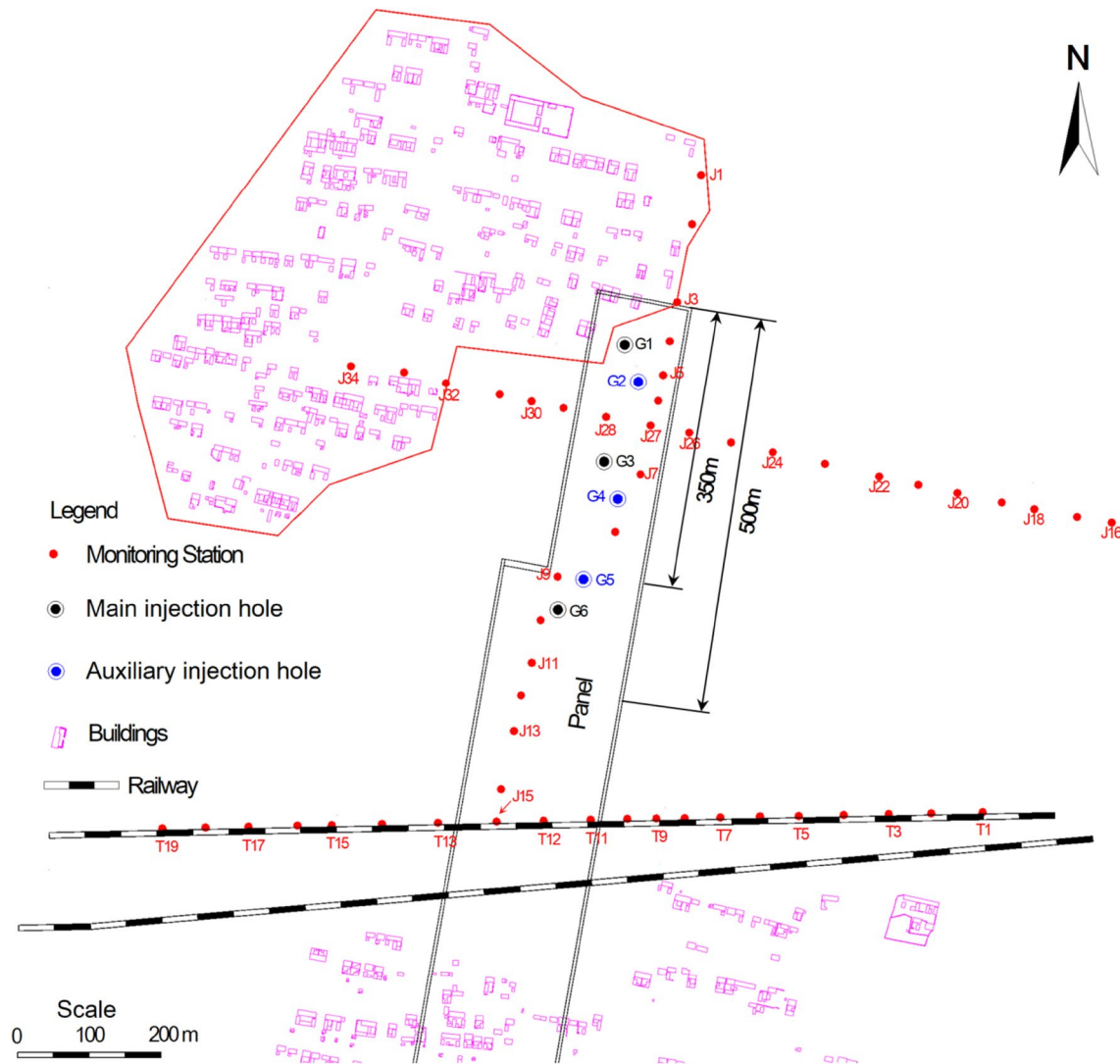|	G1	G2	G3	G4	G5	G6
Distance to the opening (m)	60	110	210	250	360	400
Distance to the tail gate (m)	75	50	75	50	75	100
Distance to the coal seam roof (m)	60	90	60	90	90	60
Borehole depth(m)	383.5	373.5	398.5	383.5	378.5	400.5
Panel elevation (m)	−425.0	−445.0	−440.0	−455.0	−450.0	−442.0

Fig. 6 Layout of surface observation stations and injection boreholes. J1–J15 is the observation line in strike direction; J16–J34 and T1–T19 in dip direction

Development of multi-bed separations and overburden grouting

When the coal seam is mined to 49 cm (245 m in prototype), the overlying strata slump in one-time. At the roof, the rock beam hinged structure appears and overlying rock is deformed and subsiding under the influence of gravity. A certain void appears in the upper strata above goaf. The immediate roof of mudstone and siltstone collapses first accompanied by rock fracture (Fig. 7b). With the panel advancing, the sixth stratum caves completely, causing microcracks in the upper rock strata (Fig. 7c). In the process of panel advances to 70 cm (350 m in prototype), the mudstone and medium sandstone are separated first at a distance of 14 cm above the roof due to the underlying mudstone stratum fracture. The bed separation has generated and

developed at 70 m in prototype above the top of the roof. The space of bed separation is in the expansion stage of the bed separation development cycle this moment and the space of bed separation is continuously increasing. In this process, overburden grouting can be started (Fig. 7d). The first stage of bed separation grouting test started at this time. During the grouting process, it shows clearly that the strata beneath the bed separation was squeezed obviously by the injecting mass (Fig. 7e). At the same time, the cracks in the overlying stratum are decreasing. This implies that the filling mass has a positive effect to support the overlying rocks. When the panel advances to 91 cm (455 m in prototype), the thicker main roof is broken, the vertical fissure breaks through the lower medium sandstone stratum and propagates upward. As the bed separation continues to develop to 16.8 cm (84 m in prototype), cracks and bed separation are formed
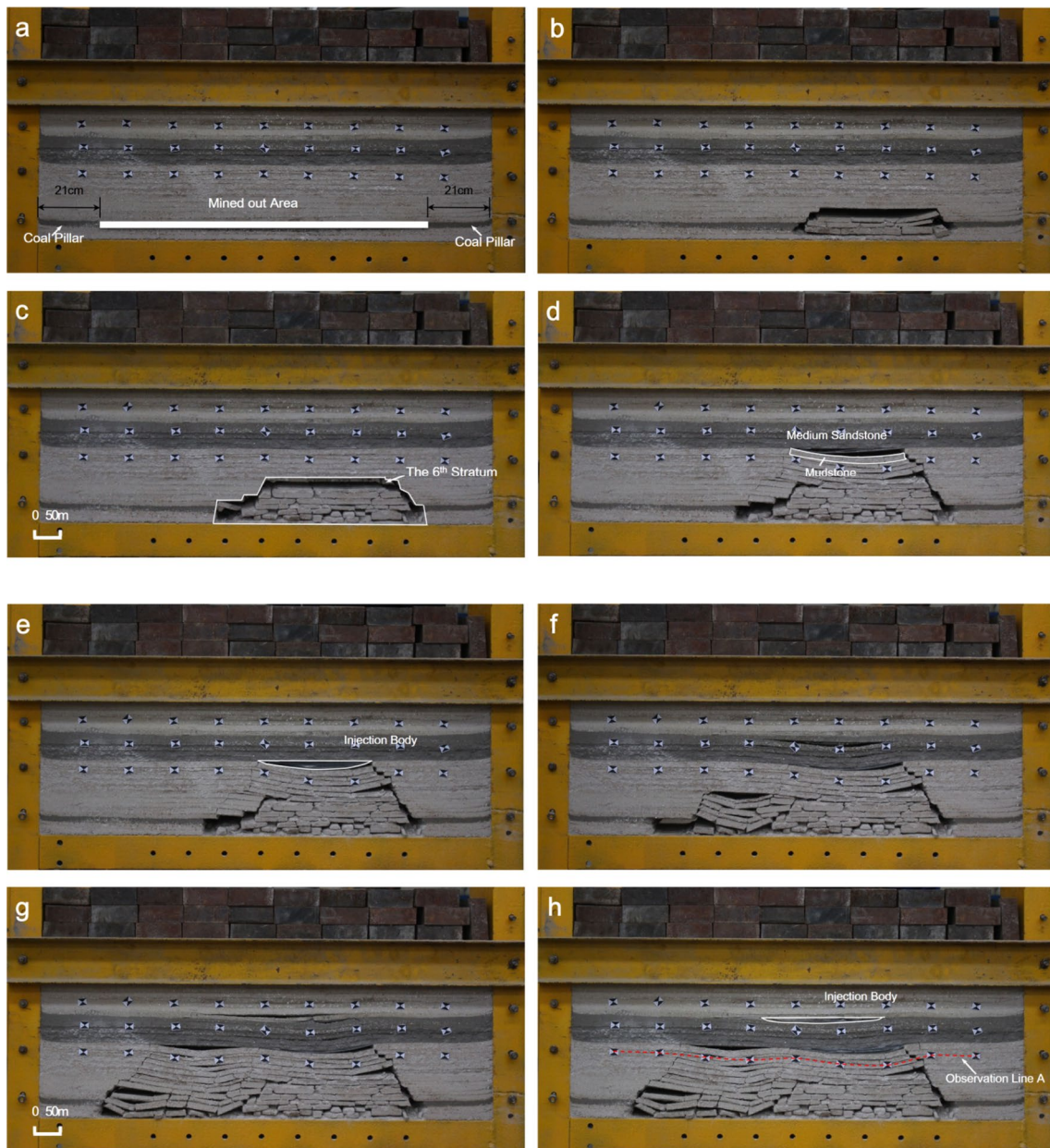
Fig. 7 Overburden movement, occurrence of bed separation and grouting

in the upper part above the goaf (Fig. 7f). When the panel is advanced to 98 cm (490 m in prototype), the grouting is carried out on the bed separation below the upper medium sandstone stratum. The cracks in the upper rock decreases even disappear, while the bed separation space is gradually reduced due to grouting (Fig. 7g, h).

From the scale model test, the coal seam continues to be excavated, the subsidence area gradually increases. When the grouting starts, the underlying stratum below the filling mass is gradually compacted and the cracks under the overlying rock decrease slowly. The filling mass in the middle is thicker than that on the edges due to disc-shaped separation.

The fractured rocks are more seriously compacted than that on the edges because the stress in rocks below the center of bed separation reaches the maximum. In the multi-bed separation grouting method, the injection–production ratio is larger than that in traditional overburden grouting.

Relationship between injection–production ratio and grouting quantity

The space of bed separation will be smaller than the volume of coal production because of the expansion of rocks, which will affect the grouting quantity and subsidence reduction

ratio. The excessive grouting quantity will cause surface uplift, while the opposite will lead to a low subsidence reduction. Therefore, a reasonable grouting quantity should be determined to control surface subsidence.

The injection–production ratio is defined as the ratio of injection quantity to excavated coal quantity. In the simulation of the overburden grouting by UDEC, the volume of injected slurry is controlled by setting the grouting pressure to produce a stable flow velocity of the slurry and a grouting time. The results show that the injection–production ratio increases with the increasing grouting pressure (Table 4). Figure 8 shows that the injection–production ratio has a significant effect on the control of surface subsidence. Figure 9 shows the maximum subsidence curve based on different injection–production ratios. There is a linear relationship between the maximum subsidence and the injection–production ratio. The higher the injection–production ratio means the less surface subsidence. A linear correlation with a correlation coefficient of 0.99
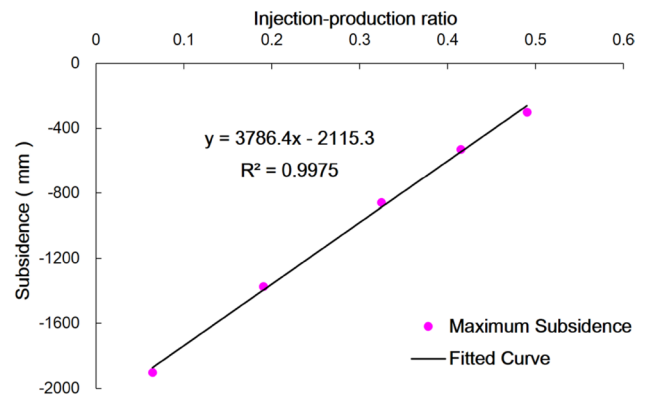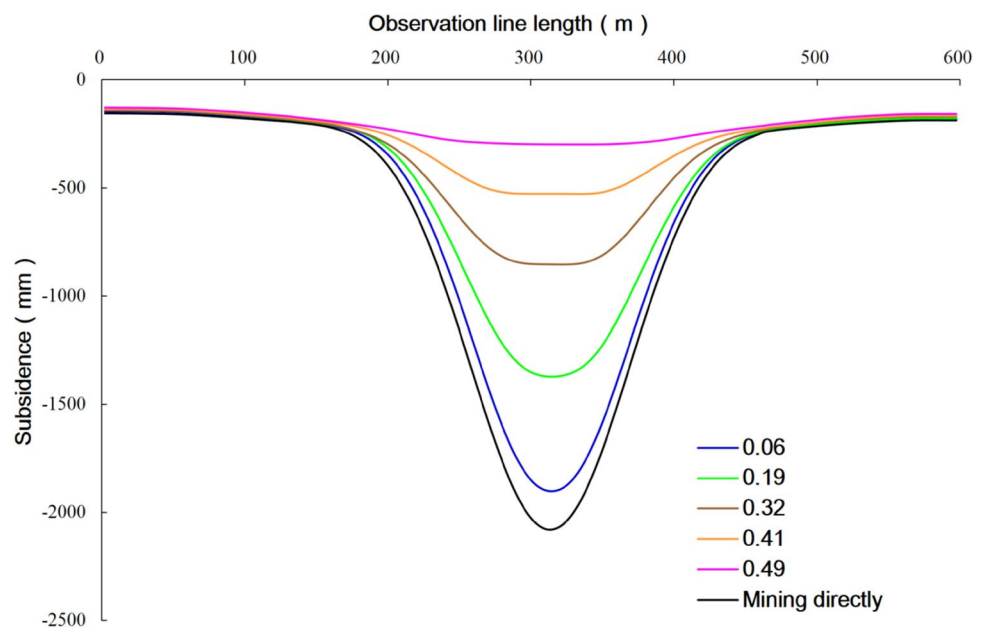

Fig. 9 The maximum subsidence of different injection–production ratios

between the injection–production ratio and the maximum surface subsidence is shown in the formula:

$$y = 3786.4x - 2115.3, \qquad (8)$$

where x is the injection–production ratio and y is the maximum subsidence.

In view of this result, the injection–production ratio of 0.45 and above is adopted to ensure that the surface deformation is within level I, which means damage to constructions is negligible and no visible cracks appeared on the walls referred to the classification of critical deformation values of surface concrete structures (Table 5). (The designed injection–production ratio can be obtained by the curves based on the requirement of subsidence reduction.)

Table 4 Injection pressure vs injection–production ratio

Injection pressure (MPa)	Injection–production ratio (in actual)
2.0	0.06
2.5	0.19
3.0	0.32
3.5	0.41
4.0	0.49

Fig. 8 Subsidence curve for different injection–production ratios

Table 5 Classification of critical deformation values of surface concrete structures (State Administration of Work Safety 2017)

Damage level	Surface movement and deformation			Classification	Structural processing
	Horizontal strain (mm/m)	Slope (mm/m)	Curvature (mm/m²)		
I	≤ 2.0	≤ 3.0	≤ 0.2	Negligible	No repairing
II	≤ 4.0	≤ 6.0	≤ 0.4	Slightly damaged	Light repairing
III	≤ 6.0	≤ 10.0	≤ 0.6	Medium damaged	Medium repairing
IV	> 6.0	> 10.0	> 0.6	Severely damaged	Heavy repairing or reconstruction

Effect of subsidence reduction

Result from scale model testing

Figure 10a shows subsidence along the observation line A in the scale model test, which lies under the lower medium sandstone stratum. When the seam is mined to 350 m, the middle and lower parts of the mudstone stratum are fractured, bed separation is formed at the bottom of the lower medium sandstone stratum, and the maximum subsidence is 489 mm. When the coal seam is mined to 490 m and excavation is completed, the bed separation tends to be closed and develops at the bottom of the lower medium sandstone stratum. At this point, the maximum subsidence in the observation line A reaches 1237 mm.

The observation line B lies between the two medium sandstone strata (Fig. 10b). When the coal seam is advanced to 350 m, the bed separation occurs under the lower medium sandstone stratum and the first grouting begins. With an increase of the filling quantity, the maximum subsidence reduces gradually, indicating that the grouts plays an important role to support the overlying rock strata. In comparison with Fig. 10a, the subsidence is effectively mitigated. When the seam is mined to 490 m, the bed separation breaks through the lower medium sandstone stratum and develops to the upper medium sandstone stratum beneath (98 m distance from the roof). Then, the maximum subsidence of the observation line B reaches 94 mm.

The observation line C is located above the upper medium sandstone stratum (Fig. 10c). When the coal seam is mined to 490 m, the upper medium sandstone stratum shows no obvious bending deformation. At this point, the maximum of the observation line C reaches only 80 mm, which indicates an effective control of subsidence.

Result from numerical simulation

Figure 11 shows the numerical simulation results. The maximum surface subsidence reaches 2082 mm without grouting. As the pressure of grouting reaches the 4.0 MPa, the injection–production ratio is 0.49 for overburden bed separation grouting (Table 4). The maximum subsidence is 298.8 mm.

High grouting pressure and filling masses overlaid increase the space of bed separation and grouting quantity, all of which indicates that multi-bed separation grouting method has a better effect on reducing surface subsidence.

Result from field measurements

Figure 12 shows the grouting pump outlet pressure of the different grouting boreholes. The grouting pressure is low initially and then gradually increases as the grouting quantity increased. The grouting pressure underwent a change from non-pressure or low-pressure to high-pressure. The results of numerical simulation show that a pressure of 4.0 MPa is the maximum grouting pressure close to the result of field grouting test.

Table 6 shows that the maximum subsidence, slope, curvature, horizontal displacement and horizontal deformation of the surface reaches 2082 mm, 10 mm/m, 0.14 mm/m², 1000 mm and 11 mm/m due to mining without grouting, respectively. Ground constructions would be damaged in level IV according to Table 5 and a heavy repair or reconstruction needed. While the maximum subsidence, slope, curvature, horizontal displacement, and horizontal deformation of the ground village are 92 mm, 0.7 mm/m, − 0.01 mm/m², 79 mm, and 0.64 mm/m due to mining with grouting, respectively (station J32 is the maximum subsidence in surface village area). The construction damage above the panel is within level I. Therefore, the surface subsidence caused by coal mining is effectively controlled (Table 6).

The experimental results are verified and evaluated for the control effect of surface subsidence in the process of grouting by surface measurements. Twenty-two times subsidence observations were conducted. The last observation shows that the villages over the panel have been in a stable state. The maximum surface subsidence with overburden grouting is 418 mm, indicating the grouting has a significant effect on subsidence control. Furthermore, the measured maximum horizontal deformation measurement in the village zone is 0.64 mm/m (as surface subsidence was strictly controlled within the level I 2 mm/m to meet the requirement).

The application of multi-bed separation grouting with a high grouting pressure and filling mass overlaid increases
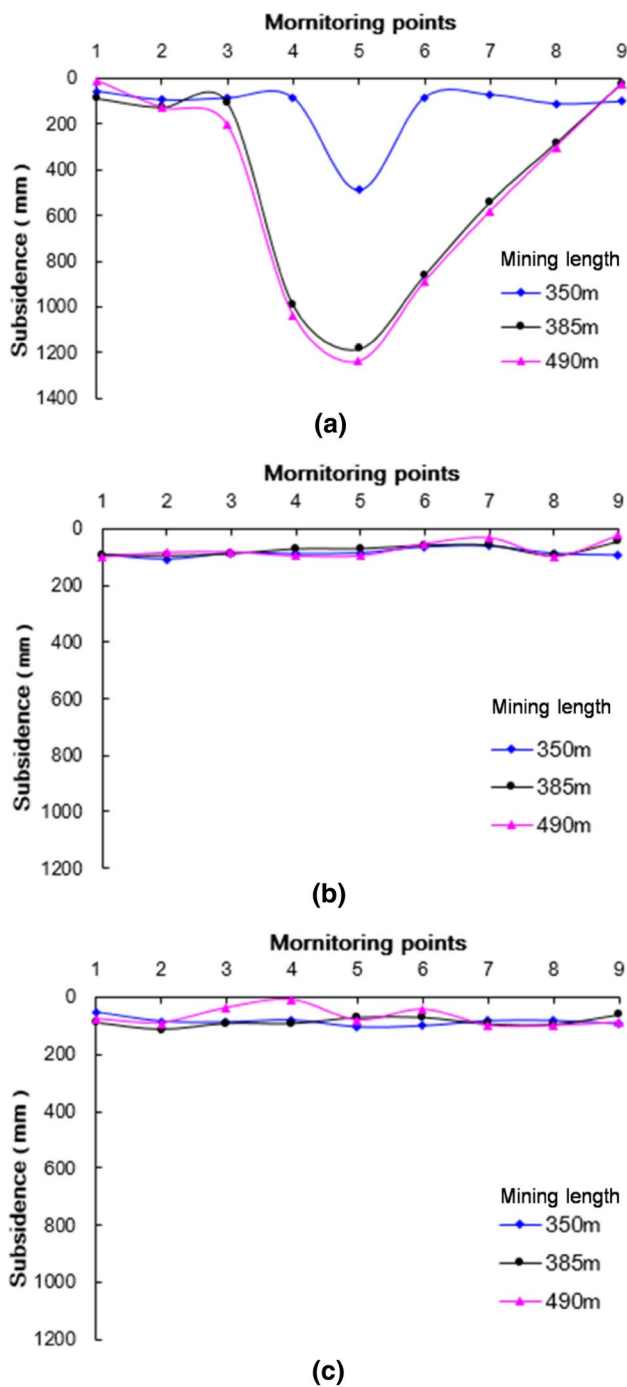
(a)

(b)

(c)

Fig. 10 Subsidence along of the observation line. **a** Line A; **b** line B; **c** line C

Fig. 11 Comparison surface subsidence of grouting and without grouting

overburden deformation and control surface subsidence without the thick and strong strata in the overburden.

Discussion

The field measurements showed that the technique can be applied in cases of small scale of bed separations developed. The multi-level filling mass can transmit the load down to the roof of the coal seam, increase the compaction of the fractured rock and expand the space of bed separation without thick and strong strata for generating large-scale bed separation.

Several coal mines in China have used traditional overburden grouting technology in this study and shown overburden grouting technique interfering little with normal excavation and improving the coal recovery rate (Teng et al. 2016; Chen et al. 2016). However, the application of overburden grouting is largely limited by geological conditions with the thick and strong strata in overburden (Sun et al. 2008). The larger space of bed separation developed under the thick and strong strata to get more grouting quantity injected and meet requirement of subsidence reduction. Moreover, the surface subsidence can be mitigated to some extent by increasing the size of pillars properly to support overlying strata (Xuan and Xu 2014; Chen et al. 2016). With overburden grouting, adjusting the width and length of panel, surface deformation and subsidence reduction can be effectively mitigated. The filling mass and coal pillars together support the overlying strata, resulting a surface subsidence coefficient of less than 0.15 (Xuan and Xu 2017).

The multi-bed separation grouting used in the Qi'nan Coal Mine improves the subsidence reduction ratio and solves the problem of low injection–production ratio without

the amount of compression of fractured rocks above seam roof. With the total injection–production ratio increased, subsidence reduction increases correspondingly to eliminate the limitation of geological conditions without obvious strong overburden strata. Field measurements verified multi-bed separation grouting can effectively mitigate
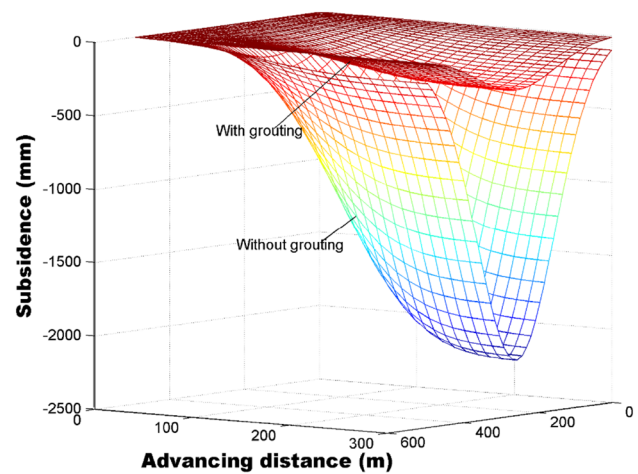
Fig. 12 Measured grouting pressure curve. G1, G3 and G6 are the main injection hole; G2, G4 and G5 the auxiliary injection hole
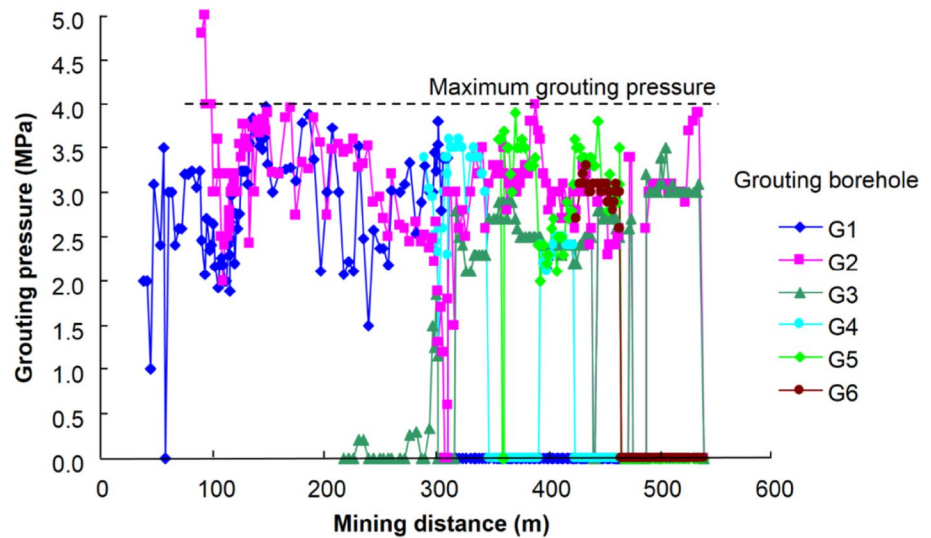

Table 6 Surface deformations with grouting and without grouting

Mining method	Subsidence (mm)	Slope (mm/m)	Horizontal strain (mm/m)	Curvature (mm/m^2)	Horizontal displacement (mm)	Damage level
Predicted (without grouting)	−2082	10.0	−11 to 5	−0.14	1000	IV
Observed (with grouting)						
Surface	−418	2.0	−2 to 2	−0.01	100	I
Station J32	−92	0.7	0.6	−0.01	79	I

thick and strong rocks in overburden, compared to the previous overburden grouting method. The multi-bed separation grouting increases the total grouting quantity and injection–production ratio. The multi-filling masses overlaid increases the load on fractured rocks above seam roof and space of bed separation developed.

The results of this study provide a helpful reference for overburden grouting in the future. However, the mechanism and effect of overburden grouting are constrained by various factors, such as grouting material, grouting technology, regional tectonics. Moreover, the grouting quantity depends largely upon the excavation speed and bed separation space. The prediction of bed separation space developed and long-term surface deformation extent of overburden grouting should also be considered in further studies.

The results of the numerical simulation and scale model testing are in good agreement with each other and the surface subsidence can be effectively mitigated. Scale modeling indicates that the overlying strata collapse periodically during excavation and bed separation goes through a cycle of "generation–development–expansion (persistence)–disappearance (compaction)" with the mining process. The injected filling material by high-pressure formed a certain size of pack supports the overlying strata. It effectively controls and mitigates the surface subsidence caused by coal mining. Numerical simulation results indicate that maximum subsidence depends linearly on the injection–production ratio.

A significant mitigation in the maximum subsidence indicates that overburden grouting is an effective way to reduce surface subsidence with a relatively small-scale bed separation developed

Conclusions

In this paper, the multi-bed separation overburden grouting method has been verified as an effective method to mitigate the overburden failure and control surface subsidence. This case study involves the Qi'nan Coal Mine in Anhui Province of China.

References

Belem T, Benzaazoua M (2008) Design and application of underground mine paste backfill technology. Geotech Geol Eng 26(2):147–174. https://doi.org/10.1007/s10706-007-9154-3

Bell FG, Stacey TR, Genske DD (2000) Mining subsidence and its effect on the environment: some differing examples. Environ Geol 40(1–2):135–152. https://doi.org/10.1007/s0025400001

Chang Q, Tang W, Xu Y, Zhou H (2018) Research on the width of filling body in gob-side entry retaining with high-water materials. Int J Min Sci Technol 28(3):519–524. https://doi.org/10.1016/j.ijmst.2017.12.016

Chen SG, Guo H (2008) Numerical simulation of bed separation development and grout injection into separations. Geotech Geol Eng 26(4):375–385. https://doi.org/10.1007/s10706-008-9174-7

Chen SG, Hu W (2009) A comprehensive study on subsidence control using COSFLOW. Geotech Geol Eng 27(3):305–314. https://doi.org/10.1007/s10706-008-9230-3

Chen S, Yin D, Cao F, Liu Y, Ren K (2016) An overview of integrated surface subsidence-reducing technology in mining areas of China. Nat Hazards 81(2):1129–1145. https://doi.org/10.1007/s11069-015-2123-x

Cundall PA, Strack ODL (1979) A discrete numerical model for granular assemblies. Geotechnique 29(1):47–65. https://doi.org/10.1680/geot.1979.29.1.47

Gray DD, Reddy TP, Black DC, Ziemkiewicz PF (1998) Filling abandoned mines with fluidized bed combustion ash grout. design and application of controlled low-strength materials (flowable fill). ASTM STP 1331:180–193. https://doi.org/10.1520/STP13071S

Itasca Consulting Group, Inc (2005) UDEC-Universal Distinct Element Code, Version 4.0-User's Guide. Itasca, Minneapolis

Jaiswal A, Shrivastva BK (2012) Stability analysis of the proposed hybrid method of partial extraction for underground coal mining. Int J Rock Mech Min Sci 52(52):103–111. https://doi.org/10.1016/j.ijrmms.2012.03.002

Karfakis MG, Bowman CH, Topuz E (1996) Characterization of coal-mine refuse as backfill material. Geotech Geol Eng 14(2):129–150. https://doi.org/10.1007/BF00430273

Li M, Zhang J, Huang Y, Zhou N (2017) Effects of particle size of crushed gangue backfill materials on surface subsidence and its application under buildings. Environ Earth Sci 76(17):603. https://doi.org/10.1007/s12665-017-6931-z

Liu J, Sui W, Zhao Q (2017) Environmentally sustainable mining: a case study of intermittent cut-and-fill mining under sand aquifers. Environ Earth Sci 76(16):562. https://doi.org/10.1007/s12665-017-6892-2

Lokhande RD, Prakash A, Singh KB, Singh KKK (2005) Subsidence control measures in coalmines: a review subsidence control in working coalmines. J Sci Ind Res 64(5):323–332 **(ipc: E 21 C 45/00)**

Loupasakis C, Angelitsa V, Rozos D, Spanou N (2014) Mining geo-hazards-land subsidence caused by the dewatering of opencast coal mines: the case study of the Amyntaio coal mine, Florina, Greece. Nat Hazards 70(1):675–691. https://doi.org/10.1007/s11069-013-0837-1

Luan H, Jiang Y, Lin H, Wang Y (2017) A new thin seam backfill mining technology and its application. Energies 10(12):2023. https://doi.org/10.3390/en10122023

Ministry of Housing and Urban-Rural Development of the People's Republic of China (2002) Code for investigation of geotechnical engineering (GB 50021-2001). China Architecture and Building Press, Beijing **(in Chinese)**

Palarski J (1989) The experimental and practical results of applying backfill. In: Proceeding of the 4th international symposium on mining with backfill. Montreal, pp 33–37

Palchik V (2003) Formation of fractured zones in overburden due to longwall mining. Environ Geol 44(1):28–38. https://doi.org/10.1007/s00254-002-0732-7

Palchik V (2005) Localization of mining-induced horizontal fractures along rock layer interfaces in overburden: field measurements and prediction. Environ Geol 48(1):68–80. https://doi.org/10.1007/s00254-005-1261-y

Rankine RM, Sivakugan N (2007) Geotechnical properties of cemented paste backfill from Cannington Mine, Australia. Geotech Geol Eng 25(4):383–393. https://doi.org/10.1007/s10706-006-9104-5

Rankine R, Pacheco M, Sivakugan N (2007) Underground mining with backfills. Soils Rocks 30(2):93–101

Shen B, Poulsen B (2014) Investigation of overburden behavior for grout injection to control mine subsidence. Int J Min Sci Technol 24(3):317–323. https://doi.org/10.1016/j.ijmst.2014.03.005

Siriwardane HJ, Kannan RSS, Ziemkiewicz PF (2003) Use of waste materials for control of acid mine drainage and subsidence. J Environ Eng 129(10):910–915. https://doi.org/10.1061/(ASCE)0733-9372(2003)129:10(910)

Sivakugan N, Rankine RM, Rankine KJ, Rankine KS (2006) Geotechnical considerations in mine backfilling in Australia. J Clean Prod 14(12):1168–1175. https://doi.org/10.1016/j.jclepro.2004.06.007

Sivakugan N, Veenstra R, Naguleswaran N (2015) Underground mine backfilling in Australia using paste fills and hydraulic fills. Int J Geosynth Ground Eng. 1:18. https://doi.org/10.1007/s40891-015-0020-8

Sroka A, Knothe S, Tajdus K, Misa R (2015) Underground exploitations inside safety pillar shafts when considering the effective use of a coal deposit. Gospod Surowcami Min 31(3):93–110. https://doi.org/10.1515/gospo-2015-27

State Administration of Work Safety (2017) Regulations for setting pillar and mining under buildings, railways and water bodies. China Coal Industry Publishing House, Beijing **(in Chinese)**

Sun W, Zhu W, Zheng X (2008) Application and development status of technology of grouting into overburden bed-separation to reduce ground subsidence. Coal Technol 27(2):81–83 **(in Chinese)**

Teng H, Xu J, Xuan D, Wang B (2016) Surface subsidence characteristics of grout injection into overburden: case study of Yuandian no. 2 coalmine, China. Environ Earth Sci 75:530. https://doi.org/10.1007/s12665-016-5556-y

Xuan D, Xu J (2014) Grout injection into bed separation to control surface subsidence during longwall mining under villages: case study of Liudian coal mine, China. Nat Hazards 73(2):883–906. https://doi.org/10.1007/s11069-014-1113-8

Xuan D, Xu J (2017) Longwall surface subsidence control by technology of isolated overburden grout injection. Int J Min Sci Technol 27:813–818. https://doi.org/10.1016/j.ijmst.2017.07.014

Xuan D, Xu J, Zhu W (2014) Dynamic disaster control under a massive igneous sill by grouting from surface boreholes. Int J Rock Mech Min Sci 71:176–187. https://doi.org/10.1016/j.ijrmms.2014.06.019

Yang P, Li L (2017) Evolution of water table and pore-water pressure in stopes with submerged hydraulic fill. Int J Geomech 17(9):1. https://doi.org/10.1061/(asce)gm.1943-5622.0000944

Yao Y, Cui Z, Wu R (2012) Development and challenges on mining backfill technology. J Master Sci Res 1(4):73–78. https://doi.org/10.5539/jmsr.v1n4p73

Yin B, Kang T, Kang J, Chen Y (2018) Experimental and mechanistic research on enhancing the strength and deformation

characteristics of fly-ash-cemented filling materials modified by electrochemical treatment. Energy Fuels 32(3):3614–3626. https://doi.org/10.1021/acs.energyfuels.7b03113

Zhang J, Zhang Q, Huang Y, Liu J, Zhou N, Zan D (2011) Strata movement controlling effect of waste and fly ash backfillings in fully mechanized coal mining with backfilling face. Min Sci Technol 21(5):721–726. https://doi.org/10.1016/j.mstc.2011.03.003

Zhu X, Guo G, Zha J, Chen T, Qi F, Yang X (2016) Surface dynamic subsidence prediction model of solid backfill mining. Environ Earth Sci 75(12):1007. https://doi.org/10.1007/s12665-016-5817-9